

TESTING OF ADVANCED CHROMIUM - IRON BASED STEEL

*J. Simeg Veternikova¹, J. Degmova¹, V. Sabelova¹, F. Simko², M. Pekarckova³, S. Sojak¹,
M. Petriska¹, V. Slugen¹*

¹Institute of Nuclear and Physical Engineering, Faculty of Electrical and Information Technology, Slovak University of Technology, Ilkovicova 3, 812 19 Bratislava, ²Department of Molten Salts, Institute of Inorganic Chemistry, Slovak Academy of Sciences, Dubravská cesta 9, 845 36 Bratislava, ³Institute of Materials Science, Faculty of Materials Science and Technology, Slovak University of Technology, Bottova 25, 917 24 Trnava

E-mail: jana.veternikova@stuba.sk

Received 30 April 2015; accepted 10 May 2015

1. Introduction

Research and Development of advanced nuclear reactors in Generation IV (GEN IV) are limited by the selection of proper construction materials. Suitable candidate materials are still under extensive investigation, because their properties must be excellent to achieve high level of reactor system safety.

NF 709 (Fe-20Cr-25Ni) is new austenitic steel with improved properties in compare to AISI steels; therefore it is also one of candidate materials. Our study is focused on investigation of radiation resistance as well as thermal stability of this steel - NF 709.

2. Experiment

Experimental samples

Austenitic steel - NF 709, manufactured by NIPPON Steel, is a candidate material for construction of pipelines, heat exchanges and reactor internal parts. The chemical composition of this steel is listed in Table 1.

Tab. 1. *Chemical composition of the investigated steels (in % wt.).*

Steels	C	Mn	Ni	Cr	Mo	Ti	Si	Nb	N	B
NF 709	0.03	0.92	25.34	22.22	1.40	0.05	0.38	0.24	0.17	0.01

This investigated steel was produced by classical process, which includes casting, cold-drawing, solution treatment at around 1100 °C and finally cold down by water quenching [1]. The samples were prepared from as-received material by cutting the steel sheets into suitable pieces. In order to remove surface impurities, the sample surfaces were polished after the cutting almost into a mirror level.

Experimental treatment and technique

The implantation experiment was performed at a linear accelerator belonging to the Slovak University of Technology. The samples were loaded by helium ions (He²⁺) with the kinetic energy up to 500 keV. The Bragg peak of the implantation is located around 950 nm according to a SRIM simulation [2]. The implantation level was ~ 1x10¹⁷ ions per cm² and the maximum radiation damage calculated for the damaged zone was around 45 dpa. During the implantation, accumulation of larger vacancy defects typical for austenitic structure was assumed in the investigated steel.

The material was also exposed to high temperature of 1000 °C during 24 hours in 99.996 % argon for purpose of thermal stability study of the steel. The thermal experiment was performed in autoclave belonging to Slovak Academy of Science. The pressure during the annealing was 8 MPa which should have simulated the pressure in nuclear reactor of Gen IV.

The samples were investigated by positron annihilation methods describing the presence of vacancy type defects in structure, namely positron annihilation lifetime spectroscopy (PALS) and positron Doppler broadening spectroscopy (DBS).

The PALS was measured in a fast-fast mode [3] with the FWHM parameter close to 220 ps. The Variance of fit (reduced chi-square) achieved value in range of $\langle 1; 1.1 \rangle$. The positron source of PALS was ^{22}Na in a Kapton foil with the energy up to 540 keV. The PALS can determine the defect size and the defect concentration up to the depth $\sim 120 \mu\text{m}$.

The DBS technique [4] with a conventional setup was applied especially for observation of a surface for the experimentally treated samples. The DBS spectra were recorded by one HPGe detector with the Gaussian resolution function of 1.24 keV. The energy window for a calculation of the S parameter was $|E\gamma - 511 \text{ keV}| < 0.83 \text{ keV}$. The positrons used in the DBS measurements are acquired from a slow positron beam [5]. This technique can study the defect profiles as a function of the positron implantation depth in the samples up to 1.6 μm . Higher positron energy causes deeper penetration of positrons into samples which is defined by the Markhov profile [6].

The annealed sample was observed by SEM due to a surface colour change after the treatment. High resolution scanning electron microscope JEOL JSM 7600F with a chemical analyzer was used for observation of an oxide layer in a cross-section of the annealed sample.

3. Result and Discussion

Steel NF 709 was investigated in three different states: as-received state (after the process of production), after the annealing for simulation of thermal strain and after the helium ion implantation for purpose of radiation resistance study. Positron annihilation lifetime spectroscopy was used for a first view of the microstructural changes due to applied strains. The PALS is sensitive for the layers up to $\sim 120 \mu\text{m}$, which is more than the implanted layers up to 1.2 μm . However around 20 % of positrons annihilate in this layer [7]; therefore if the change is significant even in this thin layer, a change of positron lifetime may also be visible. The implanted sample was studied in more detail by DBS technique studying surface and subsurface layers up to 1.6 μm .

The annealing of sample took 24 hours, thus the whole sample was influenced by the thermal strain. This experimental treatment is convenient for classic PALS study. Our assumption was that the structure can transform or new vacancy defects due to effect of thermo-vacancies can appear during annealing. The annealing was performed in very pure argon; therefore an influence of environment was not expected.

The PALS spectra were evaluated by a method of the Standard trapping model [8] in software LifeTime9 (LT9) [9], where the positron data are decomposed into 3 components - lifetimes (LT) and their intensities (I). The shortest lifetime (LT1) represents positron annihilation in the bulk (theoretical value in iron 110 ps [10]). Measured LT1 for as-received sample achieved $92 \pm 3 \text{ ps}$, annealed and implanted samples exhibit $103 \pm 2 \text{ ps}$. These values are slightly reduced (especially for as-received sample) due to a presence of defects described in second component.

The second positron lifetime (LT2) characterizes the vacancy type defects and is dependent on the size of three dimensional vacancy clusters V_n consisting of n vacancies. Its values for the investigated steels achieved between 195 and 241 ps.

The last lifetime LT3 (>500 ps) describes in-flight annihilation, i.e. annihilation in the positron source and in air between the source and the samples not fully removed by a source correction. Its intensity is neglected (1 – 2 %); therefore it is not further presented. LT3 is only used for calculation of Mean lifetime which is the value not influenced by data treatment only by measurement uncertainty ~ 2 ps.

The PALS results are shown in Fig. 1a which demonstrates only values describing defects - defect size (LT2) and defects amount proportional to intensity of positron annihilation in defects (I2). The LT2 of the as-received sample was the smallest (195 ± 12 ps) which probably indicates a presence of di-vacancies. The defects grew after the annealing (LT2 = 231 ± 18 ps) as well as due to the implantation (LT2 = 241 ± 14 ps). Both samples, annealed one as well as implanted one, contain three-vacancies in predominance.

The intensity of the defects (proportional to defect concentration) found in the as-received sample was the highest; however the defects are the smallest. After both experimental treatments, the intensities manifested a decrease ($\Delta I_2 \sim 8\%$ for annealed and 6 % for implanted sample) which was almost the same for both treatments in light of a measurement uncertainty.

The Mean lifetimes of the investigated samples achieved almost similar values. There is not any significant change after the experimental loads. Only the annealed sample showed a slight increase, which was firstly expected; however it is almost negligible due to the measurement uncertainty. The annealing had a small addition to defect accumulation in the structure.

The MLT for the as-received and implanted samples achieved value of 153 ± 2 ps, while sample after the annealing 156 ± 2 ps. The change of positron data due to the implantation was not really assumed because the classic equipment for PALS is not sensitive to surface and subsurface layers up to a few μm . The change of microstructure can be more accurately investigated by DBS measurement studying the layers up to 1.6 μm .

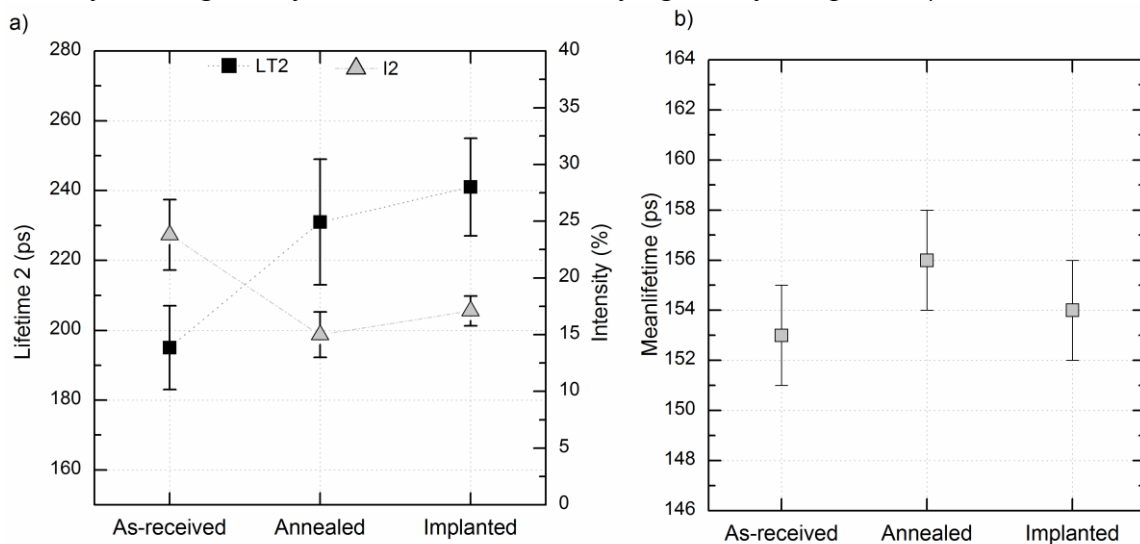


Fig.1: PALS results: Lifetime 2 proportional to defect size and Intensity describing positron annihilation in defects related to defect concentration (a), Mean lifetime proportional to defect presence (b).

The as-received and implanted samples were further observed by DBS measuring and the results are shown in line-shape parameter S. The annealed sample has not yet been studied by this technique seeing that its microstructure changed in the whole sample not only in the surface and subsurface layers. The sample of NF 709 changed the colour from metallic

one into mat black after the annealing. The annealed sample of NF 709 is covered by an oxide layer (Fig. 2); although minimal oxygen content ($< 4 \times 10^{-3} \%$) was present in the autoclave during the experiment. Chemical analyses proved a presence of chromium oxides layer with a thickness more than $2 \mu\text{m}$. Therefore DBS technique could not observe material NF 709 but only the oxide layer which was not purposive for our study.

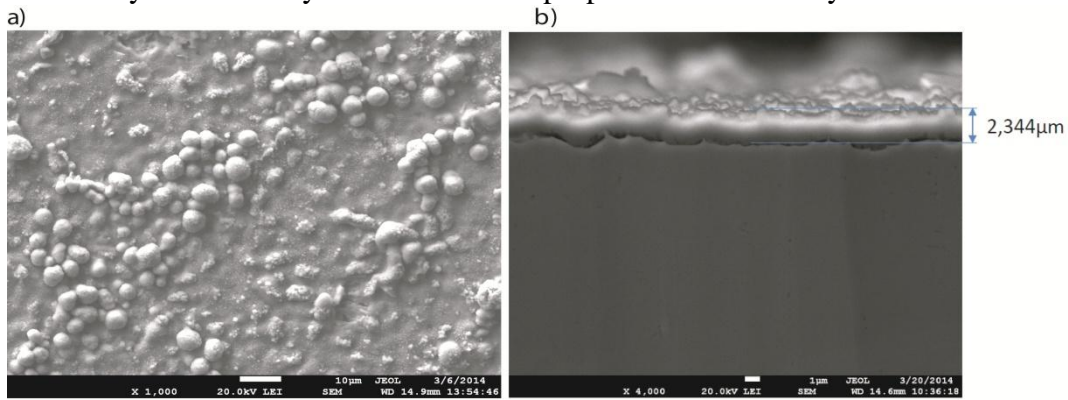


Fig.2: SEM photos of annealed NF 709: granular oxides on the surface (a), cross-section with oxide layer (b).

DBS results for the as-received and the implanted samples (Fig.3) are presented as a dependency of S parameter on positron implantation energy of positron beam, which is proportional to the implantation depth. The S parameter differs for the as-received and the implanted samples; therefore these samples have different distribution of defects in the investigated layers.

For the as-received sample the monotonous decrease of S parameter is typical indicating almost defect-free structure. The S parameter in the surface layers and up to $\sim 0.2 \mu\text{m}$ ($\sim 10 \text{ keV}$) demonstrates existence of surface defects formed during manufacturing and later a reducing influence of defects in deeper microstructure.

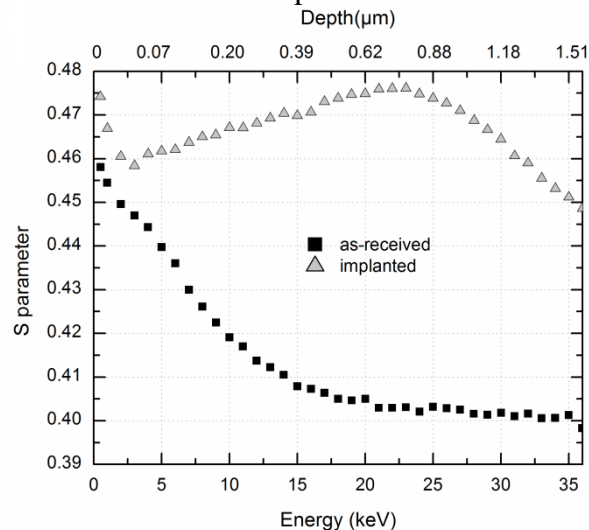


Fig.3: DBS results for as-received and implanted sample of NF 709: Defect depth profile shown by S parameter.

The S parameter for the implanted sample firstly slightly decreased due to effect of surface. Then the S parameter was increasing up to $\sim 0.75 \mu\text{m}$ ($\sim 23 \text{ keV}$) and again slowly decreasing. This is an evidence of radiation damage created by the helium implantation.

The real maximum shown as peak of S parameter was shifted closer to a surface ~ in a depth of 750 nm (~ 23 keV), while SRIM calculation estimated maximum around 950 nm.

4. Conclusion

New austenitic steel NF 709, candidate materials for construction of Generation IV reactors, was observed in term of its stability after an exposure to very high temperature and irradiation. The change of microstructure was observed by positron annihilation techniques which demonstrated the growth of vacancy defects from di-vacancies in as-received material to three-vacancies in material after the thermal and implantation treatments; although the total change of structure was very small. Thus, NF 709 showed good resistance to tested strains and according to our preliminary results. Therefore, this material could be used for high temperature applications and interchangeable components of Generation IV reactors. In further works, a combination of radiation and thermal strains will be applied together in one sample.

Acknowledgement

This work has been carried out within the framework of the EURO fusion Consortium and has received funding from the Euratom research and training programme 2014-2018 under grant agreement No 633053. The views and opinions expressed herein do not necessarily reflect those of the European Commission. Financial contributions also from Allegro project and VEGA 1/0204/13 are acknowledged.

References

- [1] T. R. Allen: Effects of Radiation on Materials ASTM Committee E-10 on Nuclear Technology and Applications, In: Proceeding of the 22nd *Symposium on Effects of Radiation on Materials*, Boston, USA, June 8-10 (2004).
- [2] J. F. Ziegler, M. D. Ziegler, J. P. Biersack, *Nucl. Instr. Meth. Phys. Res. B* **268** 1818 (2010).
- [3] M. Petriska, A. Zeman, V. Slugen, V. Krsjak, S. Sojak, *Phys. Stat. Solidi. C* **60** 2465 (2009).
- [4] R. K. Willardson, E. R. Weber, M. Stavola, Identification of Defects in Semiconductors, Academic press, Hardbound, Washington, USA (1998). ISBN-13: 978-0-12-752159-6.
- [5] J. Oila, V. Ranki, J. Kivioja, K. Saarinen, P. Hautojaervi, *Appl. Surf. Science* **194** 38 (2002).
- [6] R. Krause-Rehberg, S. H. Leipner, Positron annihilation in Semiconductors Springer Berlin Germany, 1998. ISBN 3-540-64371-0.
- [7] V. Slugen, M. Pavlovic, V. Krsjak et al., Point defects and dislocation study of alpha Fe and selected Fe-Cr alloys containing helium, Annual Report of Association Euratom CU 2008, Library and Publishing Centre, September 2009, Bratislava, ISBN 978-80-89186-57-0.
- [8] P. Hautojaervi, C. Corbel, Positron spectroscopy of solid, IOS Press Amsterdam, 1995.
- [9] J. Kansy, *Nucl. Instr. Meth. Phys. Res. A* **374** 235 (1996).
- [10] V. Slugen, Safety of VVER-440 Reactors: Barriers Against Fission Products Release, Springer, New York, 2011. ISBN 978-1-84996-419-7.